International Journal of Robotics and Mechatronics

Investigation of Machining Tool Path on Surface Roughness and Dimensional Accuracy for High-Speed Micro Milling

Amin Dadgari[†], Dehong Huo[†], David Swailes[§]

[†]Mechanical Engineering, School of Engineering, Newcastle University, Newcastle upon Tyne, NE1 7RU, UK

[§]School of Mathematics, Statistics and Physics, Newcastle University, Newcastle upon Tyne, NE1 7RU, UK

Abstract**—**This paper investigates the effects of machining tool path and cutting layer strategies on machining efficiency and accuracy in micro-milling of linear and circular micro-geometric features. Although micro-milling includes many characteristics of the conventional machining process, detrimental an effect in downscaling the process can be excessive tool wear which could, in turn, increase the machining forces and hence affect the geometrical accuracy and surface roughness. Most of the research in micro milling reported in the literature has focused on optimising machining parameters, such as feed rate and depth of cut to achieve lower cutting forces, better surface roughness, and better machining efficiency. However, is there yet little known about the effect and stability of machining tool paths and cutting layers strategies for the micro-milling process. Various tool path strategy, including lace(0°), lace(45°), lace(90°), concentric and waveform in producing linear and circular micro geometric features were compared and analysed. The effect of various cutting layer strategies in producing thin walled structure was investigated. The optimisation method with respect to surface roughness and dimensional accuracy is proposed for selection of optimum machining strategies experimentally tested. Experimental results show that the most commonly used strategy lace(0°) and concentric, reported in the literature have provided the least satisfactory machining performance, while the waveform strategy provides the best balance of machining performance for both linear and circular geometries. Adopting an optimum sequence of material removal layer in micromachining of thin walls has proven to improve the overall accuracy. This paper concludes that an optimal choice of machining strategies in process planning is as important as balancing machining parameters to achieve desired machining performance.

Keywords**—**Micro milling, tool path strategies, thin wall structure, optimisation, process planning.

DOI: 10.21535/ijrm.v4i1.956

I. Introduction

The nature of manufacturing has changed to reflect the advancement on customer demand for high production rate, process efficiency, and product accuracy[1]. The ongoing tendency for miniaturisation of products to satisfy the modern manufacturing demand leads to new requirements that are not feasible with current manufacturing technologies[2, 3]. Strong desire for direct manufacturing of 3D geometric features with a wider choice of materials including the use of metallic material, and economic manufacturing has been on demand by micromanufacturing industries such as medical devices and micro-molds. The characteristic of material removal shows a significant difference at micro/mesoscale, and differences are the consequence of scaling down between the principal constituents of cutting operation performed, although kinematically is similar to conventional milling[4]. Current tool manufacturing restriction leads to micro tool cutting edge radius that is comparable with the size of part geometry.In addition available equipment cannot achieve an optimum machining parameter required for micro tools at an affordable cost[5]. In micro milling, the cutting process is described as the transition from cutting dominated to a ploughing-cutting process where the tool edge radius has a significant effect once uncut chip thickness falls below the tool edge radius known as minimum chip thickness [6]. Minimum chip thickness has been stated to overrule the material removal behaviour[7] in the process of downscaling affecting the surface roughness of finished part. Hence surface roughness has been used as one of the main references to evaluate the micro-milling process and selection of appropriate machining parameter [8-10].Meng & Li[11] suggested that are only four machining parameters which mainly affect the surface roughness(R_a)namely; spindle speed, feed rate, axial depth of cut and the length of the cutting tool. The rational gray analysis was used to identify the relational degree of each parameter in reference to surface roughness(R_a), suggesting feedrate and axial depth of cut have the most and cutter length has the least effect. Bandapalli et al.[9]studied the influence of feedrate and axial depth of cut using Taguchi method confirming the lower feedrate and a smaller depth of cut provides a better surface finish due to more stable machining environment. Fu et al.[12] proposed a feedrate optimisation method by analysing the cutting forces along the toolpath and utilising Newton-Raphson iteration algorithm to alter the feedrate in the original tool path file to achieve a constant feedrate and steady machining. Mayor et al.

Corresponding author: Amin Dadgari (e-mail: a.dadgari1@ncl.ac.uk).
This paper was submitted on April 1, 2017; revised on May 9, 2017; and accepted on August 31, 2017.

[13] also developed a variable feedrate intelligent segmentation method to compensate for inconsistency feedrate using interpolation technique applied to segments along the tool path. Pedro and Paulo[14] investigated three commercially used tool paths; continuous overlap spiral, parallel spiral, and parallel zigzag by comparing the finished surface roughness and machining time thus suggested that; constant overlap spiral provide a better machining performance in compare to others. Banerjee et al.[15] suggested circular tool path can avoid the discontinuities in the tool movement providing a consistent feedrate and smooth material removal. Further to the downscaling effect on the production of microparts using conventional process, the low rigidity of parts results in a significant increase in the deformation of both micro tool and workpiece[16]. The research was done on compensation methods to reduce the resultant machining deformation. Smith et al.[17] experimentally tested the effect of toolpath on machining of thin webs suggesting that process planning toolpath should be chosen with the recommendation that the section being machined is supported by as much unmachined workpiece as possible. Kim et al. [18] analysed the surface error due to the deflection of the cutting tool and geometrical deformation to be compensated in the toolpath planning. Chen et al.[19] proposed an active error compensation for each layer of machining. This compensation method compares the predicted deformation from the previous layer and adjusts the machining depth of cut for the next layer, suggesting that active multilayer compensation method is more efficient than full compensation method. Gao et al.[20] proposed a mirror machining deformation compensation using the location of the cutter and estimation of the tool deformation to offset the toolpath. The proposed method was experimentally tested and show an approximate 52.88% decrease in deformation in machining of the thin wall structure. Based on the above literature major limitation to widespread use of micro milling is the stability of machining operation. In tool path planning constant feedrate and engagement of tool are critical to stabilise the machining environment. Hence this paper experimentally investigates the effect of commonly used tool paths in micromachining of circular and linear geometries and the effect of different cutting layer strategies using constant feedrate by analysing surface roughness, geometric accuracy and machining time. An optimisation method is proposed to provide an optimum tool path and cutting layer strategy selection at different machining stages with an aim to improve machining efficiency and accuracy.

II. Methodology of Process Planning for High-Speed Milling

This work consists of three phases; Modeling, experiment and optimisation for optimum selection of toolpath and machining strategy by looking at four common manufacturing aims: machining accuracy, machining surface finish, productivity and balance of all three. The modelling phase used a well-established cutting force model to predict machining forces. Finite element environment was developed to assess the impact of predicted machining forces using different cutting layer strategies. Data collected on the impact of machining forces on the geometric behaviour of the test sample was analysed and used to propose optimum cutting layers strategy for low rigid parts. The second phase, the experimental phase was where the physical micromachining was conducted first to validate the cutting force model and numeric model used in modelling phase. Follow by machining of on thin wall structures using proposed cutting layer strategies and machining of linear and circular geometries using commonly used tool paths to collect necessary data on geometrical accuracy, surface roughness and machining time. Finally, optimisation method was proposed for an optimum selection of machining tool path and cutting layer strategy looking at four common manufacturing aim. **Figure 1** presents the workflow and method used in the selection of optimum Machining strategy.

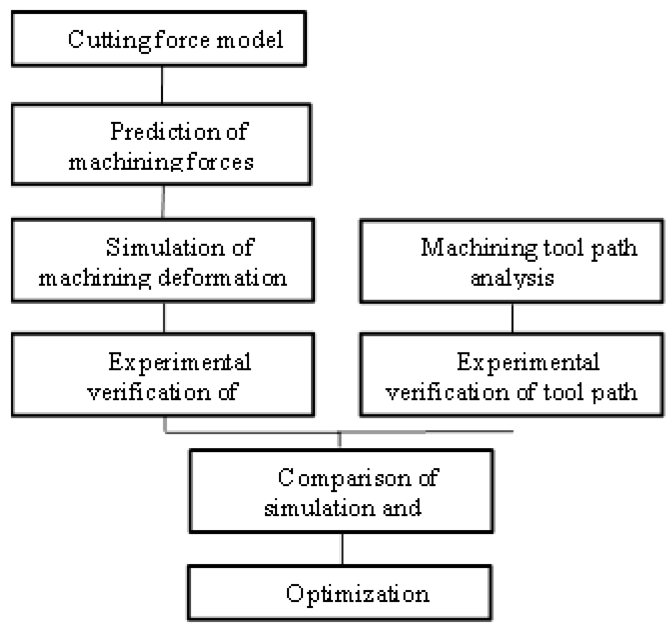

Figure 1 Flow chart of optimum machining strategies selection

III. Experimental Setup

A. Machine Tools

Experimental work has been carried out on a standard Hurco precision CNC machining center (VM10) to ensure the industrially feasible results. A high-speed spindle (NAKANISHI-HES810) with electric drive and ceramic bearings were retrofitted to the main spindle. The high-speed spindle is capable of the continuous power output of 350W and output torque of 3cNm over the speed range of 20,000-80,000rpm allowing for higher cutting velocity with smaller diameter tools. Ultra-precision collets were used to clamp the micro tool, and spindle run-out was controlled at 1μm. The machining center used to offer a single axis positioning accuracy of 5μm where the experiment has been designed to compensate for positioning error as it will be detailed in section 2.4, and will not influence the surface roughness and topography which are the main criteria of this research. Spindle error has been stated to have a significant impact on the surface roughness; in this experiment the main spindle was on mechanical lock throughout the experiment, the spindle error will be limited to the vibration and runout of the high-speed precision spindle. This experimental set up ensures that both the main spindle error such as vibration, run out and sideway error has been minimized. Therefore it will not be taken into account in the analysis.

B. Micro End Mill

Micro flat, uncoated tungsten carbide tool (WC) end mills were used in this experiment with a nominal diameter of 1 mm. A nominal tool shank diameter of 3mm used to fit 3mm ultra-precision spindle collet. Large tool diameter has been selected to prevent premature tool failure due to harsh machining environment. In each experiment, the new tool is chosen to ensure the endurance of the tool without excessive tool wear and chipping. **Figure 2** presents the geometries of selected micro end mill tool used in this experiment. Tools have also chosen from the same batch to reduce the randomization error due to the dissimilarity of the micro end mills due to different tool manufacturing techniques.

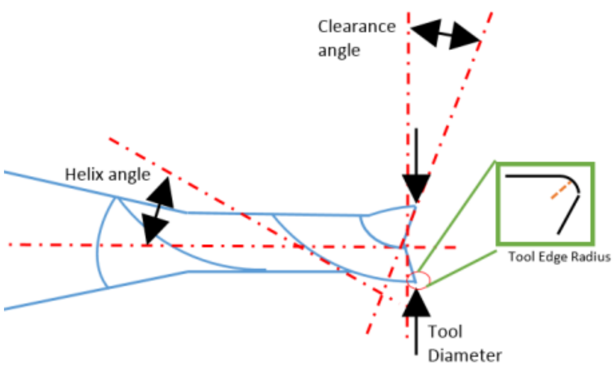

Figure 2 Micro tool geometries used in this experiment (Tool diameter: 1 mm; Number of flute: 2; Helix angle: 20 degrees; Rake angle: 0 degrees; Clearance angle: 17 degrees; and Tool edge radius: 3 µm)

C. Finite Element modelling

A numerical model of micromachining environment was developed in ANSYS to assess the impact of different machining layer strategies on the tool and low rigid micro-geometries. Explicit dynamic model of a micro cutting tool was drawn up in finite element environment to predict the deflection of cutting tool due to resultant machining forces. Johnson Cooks' material constitutive strength model was used to account for strain hardening, thermal softening and elastic recovery of the cutting tool; described in Equation (1):

$$\sigma = [A + B\varepsilon_p^n][1 + C\ln\varepsilon_p^*][1 - T_H^m], \tag{1}$$

where ε_p is an effective plastic strain, ε_p^* is normalized effective plastic strain rate and T_H is homologous temperature. The five material constant are shown in **TABLE 1**:

TABLE 1 JOHNSON-COOK'S STRENGTH MODEL CONSTANTS FOR CUTTING TOOL MATERIAL[21]

Material	*A* (MPa)	*B* (MPa)	*C*	*n*	*m*
Tungsten Carbide	770	177	0.016	0.12	1.0

Constant (A) is the initial yield stress, (B) and (n) represents the effect of strain hardening,(C) is the strain rate constant and (m) is the thermal softening exponent. Resultant cutting force (F) was applied as magnitude of F_x and F_y force in Equation (1).

$$F = \sqrt{F_x^2 + F_y^2}, \tag{2}$$

Cutting forces along the X axis, (F_x) and Y axis (F_y) in equation two have been calculated from a well-established mechanistic cutting force model adopted from Chang and Chen[22].

$$\Delta F_x(z) = \lfloor k_{tc}.h_j(\phi_j(z)) + k_{te} \rfloor \Delta L,$$
$$\Delta F_y(z) = \lfloor k_{rc}.h_j(\phi_j(z)) + k_{re} \rfloor \Delta L, \tag{3}$$

where K_{te}, K_{tc}, K_{rc} , and K_{re} are material shearing coefficients, $h_j\left(\emptyset_j(z)\right)$ is uncut chip thickness and ΔL is depth of cut. The cutting force has been experimentally validated prior to FE simulation explained in Section 4.A through machining of slots with identical machining parameters used in the experiment detailed in Section 3.A. The effect of machining forces on rigid structure was analysed by measuring maximum deformation of 30µm thin wall structures through applying static point load across the tool path illustrated in **Figure 3**.

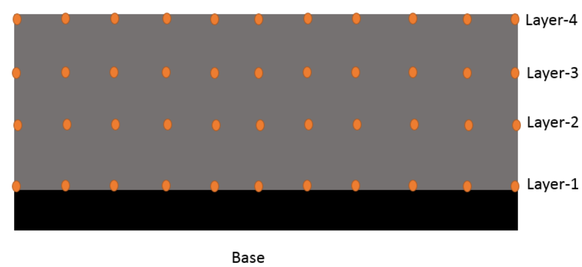

Figure 3 Point load locations across the length of thin wall

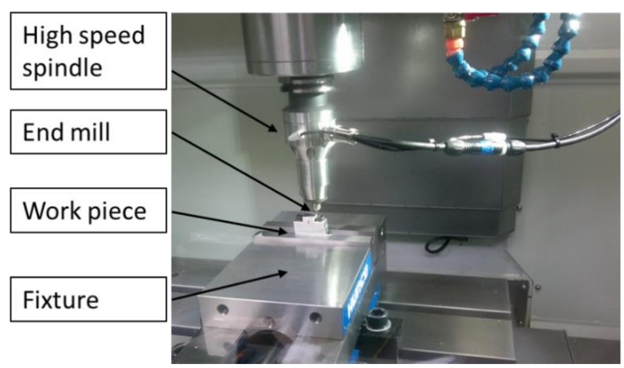

Figure 4 An illustration of experimental setup

D. Experimental procedure

In this experiment, half immersion slot milling was used to machine circular and linear geometries; **Figure 3** illustrates experiment setup on Aluminum 6061-T6, the leading non-ferrous metal in use 1mm tools were selected from a single batch to reduce the tool geometry randomization used to conduct dry milling. The surface finish and dimensional accuracy have been obtained from the experiment samples using optical 3D measurement surface profilometer; Alicona InfiniteFocusSL with a vertical resolution of 50nm. Average measurable roughness (Ra) of the machined surface recorded across the square and circular geometries. The circular geometry surfaces were scanned and flatten before average R_a could have been obtained. Machining parameter used across both experiment were; Spindle speed of 60000 RPM, radial depth of cut of 0.5 mm and 200 mm/min feed rate.The depth of cut was fixed to 2.5mm for machining toolpath experiment while machining layers strategies it varied from 1 to 3mm.

1) Machining layer strategies

Figure 5 presents a schematic diagram of selected cutting layer strategy put forward to machine 30µm thin wall structure.

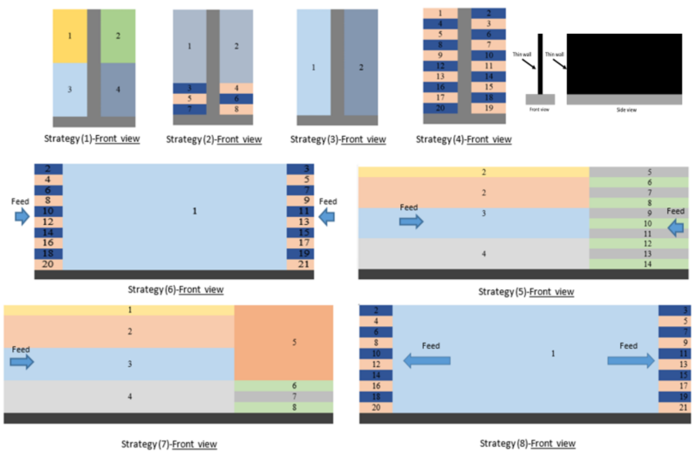

Figure 5 Schematic diagram of cutting layers strategies compared

Machining strategies 1-4 range from a full sweep of material removal across the length where strategy one proposed to remove 50% of total height of the wall from each side at each stage whereas strategy three suggest a removal of all material from one side followed by remaining on the opposite side. Strategy 4 tests the effect of a smaller layer of material removed from each side of the wall. The numerical experiment data in Section 4.B suggest a maximum geometry deformation was negligible up to 70% of material removal across the feature height. Therefore strategy 2 suggested removing 70% of material from each side with at a maximum depth of cut achieved by the micro tool follow by remaining of the material using only 10% of height per layers. Strategies five to eight, however, adopted a non continuous sweep of material removal along the length. Strategy five and seven remove 70% of material across the length and then remove the remaining uncut material at 10% of feature height layer by layer at strategy five and strategy seven propose removed 70% full height maximising the depth of cut follow the remaining material at 10% of full height layer by layer from each side. Strategy six and eight, on the other hand, propose the removal of material from the middle leaving uncut material on the end edge of the thin wall followed by removal of the remaining from each side inside to outside for strategy 8 and opposite approach on strategy 6.

2) Machining tool path

Figure 6 presents a schematic diagram of each tool path strategy used to remove the same volume of material using fixed machining parameters and machining layer strategy four presented in **Figure 5**.

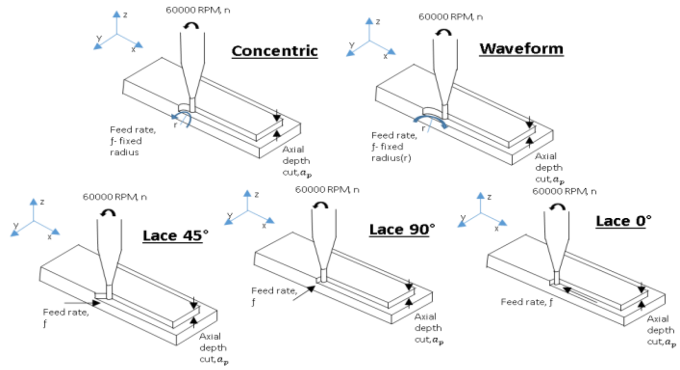

Figure 6 Schematic diagram of strategies employed in this experiment

Toolpath used in concentric strategy involves in a circular movement of the tool using constant diameter as the tool merges in and out of the material. Waveform, however, uses variable diameter toolpath as the toolpath diameter triple while the tool comes out of the material. Lace 0° follows a parallel toolpath to the finished geometry which removes the material from outer to inner layer by layer. Lace 45° and lace 90° adopted a 45° toolpath from the tangent and perpendicular to the finished geometries respectively. For both lace 45° and lace 90°, the path begins at one end of the feature and goes round the desired geometry removing all the material from outer to inner.

IV. Results and Discussion

A. Verification of cutting force model

The experiment was set up to validate the cutting forces calculated using Chang and Chen[22] mechanistic cutting force model through machining of microchannels using five different depth of cuts vary from 0.1 to 0.3 mm using matching machining parameters stated in section 2.4. Measured average cutting force across X, Y and Z is plotted in **Figure 7**. Average cutting forces obtained experimentally was compared with calculated forces presented in **Table 2**.

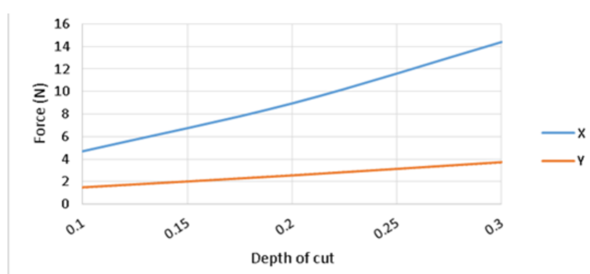

Figure 7 Average measured cutting force at various depth of cut (a_p) microchannels using 2 flutes 1mm tungsten carbide endmill

Table 2 Calculated and Measured Cutting Forces

Cutting forces	Calculated	Measured
$F_X(N)$	11.073	11.9
$F_Y(N)$	2.49	3.8

The calculated cutting forces are shown to be in good agreement with experimentally measured forces along X and Y-axis. Experimentally measured cutting force has been carried forward into numerical model FE to predict the resultant tool deflection and to predict the geometrical accuracy of the finished parts affected by tool deflection.

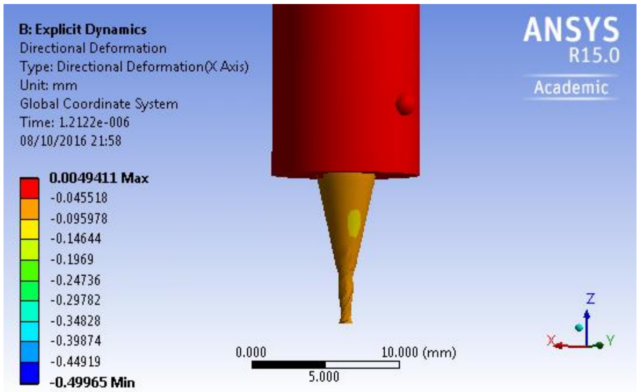

Figure 8 Micro tool deflections using numerical model

Figure 8 shows the maximum tool deflection of 0.0049mm due to experimental cutting forces, assuming there will be no deformation in the workpiece. Machining undercut of 0.0049mm from each side of the feature predicted to results in 0.0098mm in the overall geometric accuracy of the finished parts.

B. Numerical experiment of different machining layer strategies

Figures 9 and **10** show the effect of cutting forces on the geometrical accuracy of the thin wall using different proposed machining cutting layer strategies, where maximum deflection as a result of applying static force at ten equal distance across the machining path have been recorded from each side of the wall. **Table 3** presents the maximum geometry deflection predicted on the finished parts assumed to be the total plastic deformation expected.

Table 3 Numerical and experimental results in cutting layers strategies test

Strategy No.	*Avg-Geometrical deviation*	*Max-Predicted deflection (mm)*	*Max-Measured deflection(mm)*	*Machining time (Sec)*
1	-0.001	0.034	0.02075	12
2	0.003	0.035	0.068	18
3	0.028	0.035	0.096	12
4	0.008	0.035	0.042	30
5	0.053	0.034	0.089	17.4
6	0.001	0.008	0.011	16
7	0.002	0.036	0.039	13.8
8	0.004	0.035	0.043	16

Machined samples were analysed using SEM where geometrical deviation, maximum deformation and machining time from machining experiment been measured and recorded for each machining layer strategies in **Table 3**.

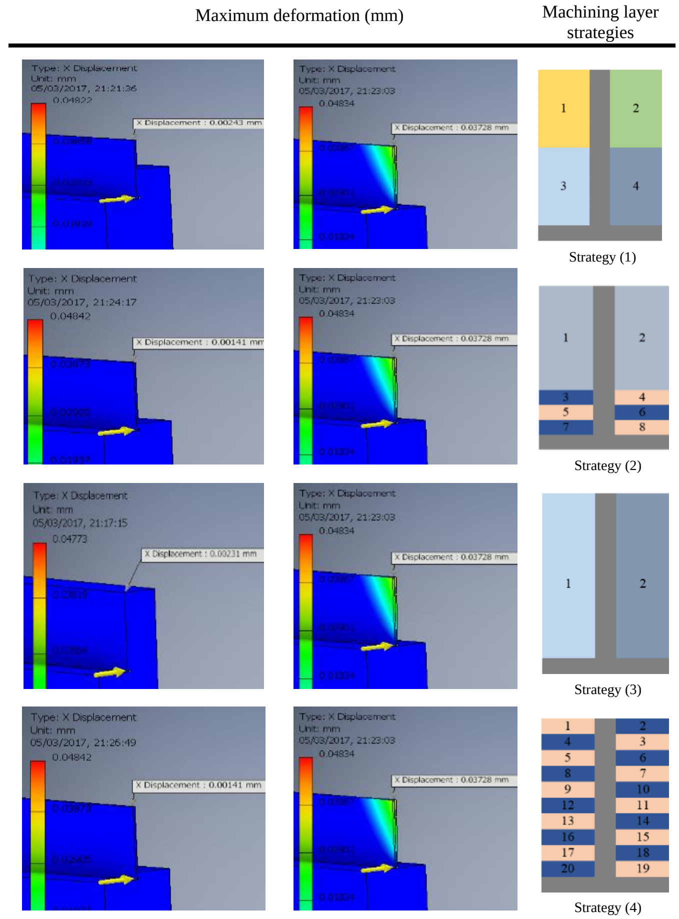

Figure 9 Machining layers strategies (continues across the length)

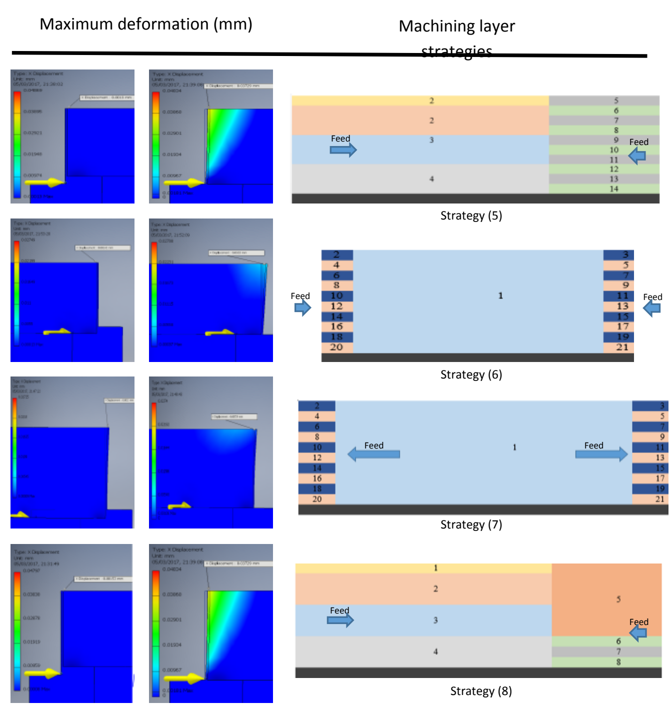

Figure 10 Cutting layer strategies numerical results with discontinuities across the length

Although the machining environment in the numerical model has been optimised to provide an accurate estimation of resultant machining deformation, the inconsistent difference between predicted and measured maximum deflection was observed. In respect to machining time strategies 1 and 3 advantage over lowest overall machining time, also leaving 50% uncut material to support the thin wall is shown to reduce maximum deflection from 0.09µm to 0.02µm significantly. However, due to the average geometrical deviation observed in strategy three being below the threshold, this strategy can be identified not suitable for micromachining. Strategies four and eight have resulted in almost the same resultant machining deflection where strategy four took nearly twice as long with significantly large geometrical deviation. Strategy two and five also have similar machining time, however, strategy two seen to be more suitable due to lower deflection and geometrical deviation. Strategy six in comparison to other strategies proposed, measured the lowest overall; deformation, average machining time and geometrical deviation. Each machining strategy has shown to be suitable for when the target of manufacturing is focused on specific tasks such as machining efficient, machining accuracy or both. Due to different machining required an optimisation method to compare and select the suitable machining layer strategy for various machining scenarios.

C. *Machining tool path strategies*

Figure 9 presents tool strategies; Lace 45°, Lace 0°, Lace 90°, concentric and waveform simulated for circular and linear geometry using EdgeCAM simulator. Data on machined surface roughness and geometrical accuracy of each machine features were measured, and machining time for each strategy was recorded and this is summarised in **TABLE 4**.

TABLE 4 EXPERIMENTALLY MEASURED DATA FOR SURFACE ROUGHNESS, ACCURACY AND MACHINING TIME

	Surface roughness(R_a) (nm)		*Geometrical deviation (mm)*		*Machining time (min)*
Strategies	**Linear**	**Circular**	**Linear**	**Circular(ϕ)**	
Lace(0)	235.084	272.0697	0.4	0.5	82
Lace(45)	296.9438	158.5829	0.4	-0.05	108
Lace(90)	298.2821	369.3157	0.1	0.1	50
Waveform	181.93	242.5562	0.02	0.3	99
Concentric	196.859	303.9412	0.5	-0.25	76

Although the machining environment in the numerical model has been optimised to provide an accurate estimate of tool deflection, the inaccuracy due to tool deflection experimentally has shown to be significantly larger. In the linear feature, the desired finished width was 10mm according to model specification. With reference to the numeric model, prediction of the finished part was predicted to be 0.0098 undercuts across all strategies providing a 10.0098 mm finish width. However, experimentally measured results have shown a significant difference summarised in **TABLE 2**. Tool strategies lace 0°, lace 45° and concentric provided a similar performance and led to the deviation of 0.4mm, 0.4mm, and 0.5mm in geometric accuracy respectively. However, lace 90° has shown a slightly better performance due to the smaller deviation of 0.1mm but still far from the predicted result. On the other hand, waveform strategy has shown a significant performance compared to the other strategies with a deviation of 0.02mm which is close enough to predict accuracy using the numeric model. In circular geometries, the desired finish diameter was also 10mm. Experimental results summarised in Table 5 show a diversity of deviations in geometric accuracy using different machining strategies. However, lace 45° and concentric strategies led to material overcut proved to be not suitable for machining of circular geometries. The deviations for geometrical accuracy lace 0° and waveform were measured to be 0.5mm and 0.3mm respectively. Nevertheless, lace 90° resulted in a significantly smaller deviation at 0.1mm shown to be more suitable for the use of machining circular geometries. The resultant surface roughness of each machining strategy was recorded in Table 5 where waveform and lace 45° provided the lowest surface roughness in machining of linear and circular geometries respectively. Machining time for each machining strategy presented in **TABLE 4** is the overall machining time including the processing time for each tool path. In this experiment due to small chip load and use of free cutting material, the tool wear assumed to be negligible.The overall machine time indicated that lace 90° is the most efficient strategy compared to the rest scored the lowest machining time of 50 min while lace 45° showed to be the least efficient strategy, scored the longest machining time of 108 min. The machining time also includes the time the CNC machine takes to process the tool path that would include cutting time. Small Due to different design requirements, an optimisation method has been adopted[14] to identify the most suitable strategy for both circular and linear geometries accordingly.

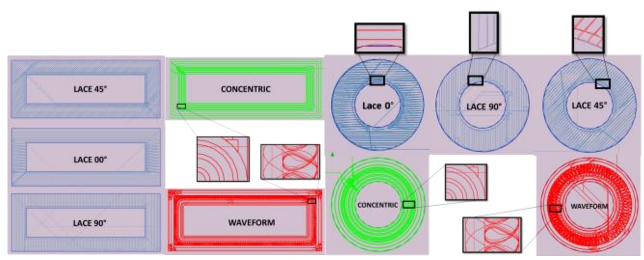

Figure 11 Machining strategies experimentally tested: (a) toolpath strategies on linear geometries; (b) toolpath strategies on circular geometries

D. *Optimization*

Machining strategies were compared with reference to geometrical accuracy and machining time. Also, machining tool paths were compared with reference to surface roughness while machining layer strategies were compared in reference to maximum deformation. A mathematical formulation as a function of all references was developed:

$$f(\alpha,\beta,\gamma)=1/\left(x(\alpha/\alpha_{\max})+x(\beta/\beta_{\max})+x(\gamma/\gamma_{\max})\right), \quad (4)$$

where x,y and z are the weight factors to add up the contribution accuracies(α), the surface roughness(β) and machining time(γ). The optimisation process approaches by evaluating the machining strategies to which variable the customer/engineer wants more, then add up the contributions and look for biggest total given. **Table 5** presents weight factors looking at four global design requirement aim to achieve; High geometric accuracy, Low surface roughness at tool path selection and maximum deflection at cutting layer strategy selection, high productivity and the combination of all of criteria's.

Table 5 Weight factors targets at each manufacturing aims

Criteria	α	β	γ
Accuracy	0.5	0.25	0.25
Surface finish/maximum deflection	0.25	0.5	0.25
Machining time	0.25	0.25	0.5
Balance	0.33	0.33	0.33

Scores for different weights based on design requirement for each scenario were evaluated and recorded in **Table 6** and **7** for both cutting tool path selection and cutting layers strategy selection; higher score indicates a better performance and suitability of the strategies for a given weights.

Table 6 Toolpath strategies scores for different weighting of each scenario

	Design Requirement			
Toolpath Strategies	**Accuracy**	**Surface Finish**	**Machining Time**	**Balance**
WAVEFORM	1.22	1.40	1.28	1.30
LACE (0)(BR)	1.14	1.22	1.22	1.19
LACE (45)	1.10	1.21	1.09	1.13
LACE (90)	1.18	1.17	1.39	1.24
CONCENTRIC(TR)	1.19	1.27	1.29	1.25

Table 7 Cutting layers strategies scores for different weighting of each scenario

	Design Requirement			
Machining Layers Strategies	**Accuracy**	**Machining Deformation**	**Machining Time**	**Balance**
1	4.71	6.13	3.87	4.73
2	1.93	2.81	2.03	2.20
3	1.37	1.63	1.72	1.56
4	1.98	2.30	1.55	1.89
5	1.17	1.14	1.30	1.20
6	5.25	5.92	3.36	4.57
7	3.08	4.24	2.74	3.24
8	3.05	4.25	2.93	3.32

The score **Table 6** shows the ranking of each tool path strategy based on each design requirements, geometric accuracy, surface roughness and machining time, individually where suitable strategies can be chosen when each of above criteria has a higher priority on design specification. The balance column presents the ranking when a balance of all criteria is requested in the design specification. Given that geometrical accuracy and surface roughness the target of product design specification, Waveform strategies are most suitable since it scored highest at 1.22 and 1.40 respectively. Providing the productivity is the goal, Lace 90° would be the suitable strategy to be used with a score of 1.39. In the scenario where design specification requests a balance of all criteria, waveform scored the highest at 1.30. The impact of various tool path strategies has shown to be more significant in machining of circular geometries where compare to linear geometries due to the wide range of scores for each criterion. Considering different manufacturing goal's, in both cases of high accuracy and low surface roughness criterion waveform has scored the highest. However this trend changed when the optimisation goal focused on productivity, Lace 90 identified to be most suitable whereas waveform was the least desired tool path to be used. The score **Table 7** presents the ranking of each machining layer strategies providing the goal of manufacturing is to have a balance of all the criteria's, strategy 1 scored the most suitable. However, since the geometrical deviation in **Table 3** indicate the finished geometry was over cut this would be the least suitable choice. Strategy 3,4 and 5 had a very similar performance all remain non-competence with strategies 6- 8. Providing the strategies feature from continues the sweep of material removal have not scored high enough to compete with others indicates conventional machining layer strategies are not suitable to be directly downscaled and used at micro scale. Strategies 7 and 8 has a noticeably high score for all criteria. However, strategy 6 scored the highest for all criteria's suggesting at process planning for micro milling leaving the uncut material at the weakest point of the geometries to be machined at last will improve the overall machining performance.

V. Conclusion

This paper presents an experimental investigation of different machining strategies and the usefulness of an integrated toolpath and machining layers strategy optimisation methodology for a high-performance micro end milling of Aluminum 6061-T6. The proposed optimisation model provides an optimum tool path and cutting layer strategy selection based on machined part requirement. The following conclusion can be drawn from this work:

- Choosing optimal machining strategies is as equally important as choosing an optimum machining parameter to achieve the overall goal of optimum machining performance and productivity.
- In process planning of machining tool path, the strategy has to be chosen taken into account feature part geometry.
- Different machining layer strategies result in variation of geometric deformation wherein machining of low rigid feature the material removal should proceed from the least supported location to most supported location
- Low surface roughness and high accuracy currently are achieved at the expense of productivity, however in process planning by selection of suitable machining strategy a balance of high-performance machining and productivity can be accomplished.

REFERENCES

[1] Lauro, C.H., et al., Optimization of micro milling of hardened steel with different grain sizes using multi-objective evolutionary algorithm. Measurement, 2016. 85: p. 88-99. CrossRef

[2] Weule, H., V. Hüntrup, and H. Tritschler, Micro-Cutting of Steel to Meet New Requirements in Miniaturization. CIRP Annals - Manufacturing Technology, 2001. 50(1): p. 61-64. CrossRef

[3] Geiger, M., et al., Microforming. CIRP Annals-Manufacturing Technology, 2001. 50(2): p. 445-462. CrossRef

[4] Dhanorker, A. and T. Ozel, Meso/micro scale milling for micro-manufacturing. International Journal of Mechatronics and Manufacturing Systems, 2008. 1(1): p. 23-42. CrossRef

[5] Okazaki, Y., N. Mishima, and K. Ashida, Microfactory - Concept, history, and developments. Journal of Manufacturing Science and Engineering, Transactions of the ASME, 2004. 126(4): p. 837-844. CrossRef

[6] Lucca, D.A., Y.W. Seo, and R.L. Rhorer, Energy dissipation and tool-workpiece contact in ultra-precision machining. Tribology transactions, 1994. 37(3): p. 651-655. CrossRef

[7] Koç, M. and T. Ozel, Micro-manufacturing: Design and Manufacturing of Micro-products. 2011: John Wiley & Sons. CrossRef

[8] Kiswanto, G., D.L. Zariatin, and T.J. Ko, The effect of spindle speed, feed-rate and machining time to the surface roughness and burr formation of Aluminum Alloy 1100 in micro-milling operation. Journal of Manufacturing Processes, 2014. 16(4): p. 435-450. CrossRef

[9] Bandapalli, C., et al., Experimental investigation of machinability parameters in high-speed micro-end milling of titanium (grade-2). International Journal of Advanced Manufacturing Technology, 2016. 85(9-12): p. 2139-2153. CrossRef

[10] Zhang, X., et al., Cutting forces in micro-end-milling processes. International Journal of Machine Tools and Manufacture, 2016. 107: p. 21-40. CrossRef

[11] Meng, H. and X. Li. Grey relational analysis for impact factors of micro-milling surface roughness. in 2015 IEEE 12th International Conference on Electronic Measurement and Instruments, ICEMI 2015. 2016.

[12] Fu, Z., et al., Feedrate optimization of complex surface milling based on predictive model of cutting force. Zhongguo Kexue Jishu Kexue/Scientia Sinica Technologica, 2016. 46(7): p. 722-730.

[13] Mayor, J.R. and A.A. Sodemann, Intelligent tool-path segmentation for improved stability and reduced machining time in micromilling. Journal of Manufacturing Science and Engineering, Transactions of the ASME, 2008. 130(3): p. 0311211-03112113. CrossRef

[14] Cardoso, P. and J.P. Davim, Optimization of surface roughness in micromilling. Materials and Manufacturing Processes, 2010. 25(10): p. 1115-1119. CrossRef

[15] Banerjee, A. and E.V. Bordatchev, Effect of circular tool path on cutting force profile in micro-end-milling. Proceedings of the Institution of Mechanical Engineers, Part C: Journal of Mechanical Engineering Science, 2012. 226(6): p. 1589-1600. CrossRef

[16] Abdolvand, H., et al., A novel combined severe plastic deformation method for producing thin-walled ultrafine grained cylindrical tubes. Materials Letters, 2015. 143: p. 167-171. CrossRef

[17] 17. Smith, S. and D. Dvorak, Tool path strategies for high speed milling aluminum workpieces with thin webs. Mechatronics, 1998. 8(4): p. 291-300. CrossRef

[18] Kim, G.M., B.H. Kim, and C.N. Chu, Estimation of cutter deflection and form error in ball-end milling processes. International Journal of Machine Tools and Manufacture, 2003. 43(9): p. 917-924. CrossRef

[19] Chen, W., et al., Deformation prediction and error compensation in multilayer milling processes for thin-walled parts. International Journal of Machine Tools and Manufacture, 2009. 49(11): p. 859-864. CrossRef

[20] Gao, S., et al., Research on specific cutting energy and parameter optimization in micro-milling of heat-resistant stainless steel. The International Journal of Advanced Manufacturing Technology, 2017. 89(1): p. 191-205. CrossRef

[21] Holmquist, T.J., D.W. Templeton, and K.D. Bishnoi, Constitutive modeling of aluminum nitride for large strain, high-strain rate, and high-pressure applications. International Journal of Impact Engineering, 2001. 25(3): p. 211-231. CrossRef

[22] Chang, Z. and Z.C. Chen, An Accurate and Efficient Approach to Three-Dimensional Geometric Modeling of Undeformed Chips for the Geometric and the Physical Simulations of Three-Axis Milling of Complex Parts. Journal of Manufacturing Science and Engineering, 2015. 138(5): p. 051010-051010. CrossRef